

To appear in *Astrophysical Journal* 478 (March 20, 1997)

THE GALACTIC DIFFUSE GAMMA-RAY SPECTRUM FROM COSMIC-RAY PROTON INTERACTIONS

Masaki Mori^{1,2}

NASA / Goddard Space Flight Center, Greenbelt, MD 20771

ABSTRACT

A new calculation of the Galactic diffuse gamma-ray spectrum from the decay of secondary particles produced by interactions of cosmic-ray protons with interstellar matter is presented. The calculation utilizes the modern Monte Carlo event generators, HADRIN, FRITIOF and PYTHIA, which simulate high-energy proton-proton collisions and are widely used in studies of nuclear and particle physics, in addition to scaling calculation. This study is motivated by the result on the Galactic diffuse gamma-ray flux observed by the EGRET detector on the Compton Gamma-ray Observatory, which indicates an excess above about 1 GeV of the observed intensity compared with a model prediction. The prediction is based on cosmic-ray interactions with interstellar matter, in which secondary pion productions are treated by a simple model. With the improved interaction model used here, however, the diffuse gamma-ray flux agrees rather well with previous calculations within uncertainties, which mainly come from the unobservable demodulated cosmic-ray spectrum in interstellar space. As a possible solution to the excess flux, flatter spectra of cosmic-ray protons have been tested and we found that the power-law spectrum with an index of about $-(2.4 \sim 2.5)$ gives a better fit to the EGRET data, though the spectrum is not explained completely.

Subject headings: cosmic rays — gamma rays — interstellar medium

1. Introduction

Observations of diffuse gamma-ray emission from the Galactic plane give us some knowledge on Galactic cosmic-rays, interstellar medium and interaction between them. The observed features, most recently by the Energetic Gamma Ray Experiment Telescope (EGRET) on the Compton

¹On leave of absence from Department of Physics, Miyagi University of Education, Sendai, Miyagi 980, Japan

²E-mail address: m-mori3@ipc.miyakyo-u.ac.jp

Gamma-Ray Observatory, are described fairly well by a model based on dynamic balance and realistic interstellar matter and photon distributions (Hunter et al. 1996).

However, the observed intensity exceeds the model prediction by as much as 60% for energies above about 1 GeV. One of the possible explanation of this discrepancy is that the theory of diffuse gamma-ray production may not be adequate at high energies: astrophysical gamma-rays above 1 GeV have never been measured before with high statistical accuracy (Hunter et al. 1996).

There are three basic components for the production of Galactic diffuse gamma-rays: nuclear interactions between cosmic-rays and matter, bremsstrahlung collisions between electrons and matter, and inverse Compton scattering of electrons with low-energy photons. Above about 200 MeV, the first component, more specifically the gamma-ray production from the decay of neutral pions produced in cosmic-ray (protons and nuclei) collisions with interstellar matter, is known to be the dominant one. Previous works on this component used isobaric models and scaling models for the nuclear interaction: see Dermer (1986a) for detail. These studies, however, were focused on lower energies. This is natural since the gamma-ray spectrum from pion decay has a peak around 70 MeV and drops rapidly toward higher energies. In order to compare the observed high-energy diffuse gamma-ray emission with model predictions, however, it is necessary to use more detailed models which describe high-energy proton-proton (p - p) collisions more accurately. Here we use Monte Carlo event generators that are commonly used in the analysis of high-energy physics experiments to simulate such collisions. We apply these results for the calculation of the Galactic diffuse gamma-ray flux from cosmic-ray interactions up to 10^7 GeV and compare it with previous studies and data from the EGRET detector.

2. Gamma-ray production in cosmic-ray interaction

The gamma-ray production source function from nuclear interaction, or the gamma-ray spectrum resulting from pion decay in p -Hydrogen atom collisions, is given by Stecker (1970)

$$\begin{aligned}
 q(E_\gamma) &= 4\pi n_H \int_{E_\gamma+m_\pi^2/4E_\gamma}^{\infty} dE_\pi \cdot 2 \int_{T_p^{\min}(T_\pi)}^{\infty} dT_p \frac{j_p(T_p)}{\sqrt{E_\pi^2 - m_\pi^2}} \frac{d\sigma(T_p, T_\pi)}{dT_\pi} \\
 &= 4\pi n_H \int_{T_p^{\min}}^{\infty} dT_p j_p(T_p) \langle \zeta \sigma_\pi(T_p) \rangle \\
 &\quad \times \int_{E_\gamma+m_\pi^2/4E_\gamma}^{\infty} dE_\pi \frac{2dN(T_p, T_\pi)/dT_\pi}{\sqrt{E_\pi^2 - m_\pi^2}}
 \end{aligned} \tag{1}$$

where the cosmic-ray proton flux is denoted by $j_p(T_p)$ [$\text{cm}^{-2}\text{s}^{-1}\text{sr}^{-1}\text{GeV}^{-1}$], $d\sigma(T_p, T_\pi)/dT_\pi$ is the differential cross section for the production of a π^0 with kinetic energy T_π in the Galactic (rest) system due to a collision of a cosmic-ray proton of kinetic energy T_p with a H atom at rest, E_π is the total pion energy and m_π is its mass, and n_H is the atomic hydrogen density. $T_p^{\min}(T_\pi)$ is the minimum proton kinetic energy that contributes to the production of a pion with energy T_π . It can be calculated from the kinematics easily. Following Dermer (1986a), we write

$d\sigma(T_p, T_\pi)/dT_\pi = \langle \zeta \sigma_\pi(T_p) \rangle dN(T_p, T_\pi)/dT_\pi$, where $\langle \zeta \sigma_\pi(T_p) \rangle$ is the inclusive cross section for the reaction $p + p \rightarrow \pi^0 + \text{anything}$ (ζ is the π^0 multiplicity) and $dN(T_p, T_\pi)/dT_\pi$ is the normalized π^0 spectrum:

$$\int_0^\infty dT_\pi \frac{dN(T_p, T_\pi)}{dT_\pi} = 1. \quad (2)$$

2.1. Secondary pion production

We studied the three Monte Carlo programs HADRIN (Hänssgen and Ranft 1986), PYTHIA (Stöstrand 1994), and FRITIOF (Pi 1992), in comparison with the scaling model of the π^0 production cross section by p - p interaction given in an analytical form by Stephens and Badhwar (1981). This scaling model was used in some of the previous calculations (Stephens and Badhwar 1981; Dermer 1986a).

The first program, HADRIN, focuses on a threshold and resonance behavior of inelastic hadron-nucleon interactions and uses tabulated cross sections for many possible reaction channels based on experimental data. It focuses on describing the nuclear collision at laboratory energies below 5 GeV. Fig. 1 shows the comparison of the simulated π^0 kinetic energy spectrum with experimental data and analytic calculations based on the isobar model (Stecker 1970) and the scaling model (see also Dermer 1986a) in the center-of-mass system (CMS). Also shown in Fig. 2 is the same data but in laboratory system (LS). One can see both HADRIN and the isobar model calculations show good agreement with experimental data within limited statistical accuracy of the data.

The program called PYTHIA³ focuses on high-energy p - p colliders and its performance is reported in detail (Sjöstrand and van Zijl 1987). This is based on a string-fragmentation model, but incorporates low transverse momentum (p_T) interactions, which is our main concern. Its usefulness for fixed target experiments, the situation similar to ours, is not fully studied, however. The other program, FRITIOF,⁴ implements a model for low- p_T hadron-hadron, hadron-nucleus and nucleus-nucleus reactions which treats a hadron as a string-like object with its color force field stretching like a vortex line. A detailed description of the model and its comparison with experimental data are reported (Andersson, Gustafson and Pi 1993).

Here we compare their predictions with the p - p collision data: due to the experimental difficulty in obtaining π^0 spectra in high-multiplicities, we use gamma-ray spectra.

Fig. 3 shows the CMS rapidity ($y^* \equiv \frac{1}{2} \ln \frac{E^* + p_L^*}{E^* - p_L^*}$, where E^* is the pion energy in CMS and p_L^* the longitudinal momentum in CMS) distributions for beam momenta of 12.4, 205, and 300 GeV/c. Data are obtained in bubble chamber experiments at Argonne (Jaeger et al. 1975a)

³ We used PYTHIA version 5.718 with JETSET version 7.408.

⁴ We used FRITIOF version 7.02 with ARIADNE version 4.02R and JETSET version 7.3.

and Fermilab (Jaeger et al. 1975b; Sheng et al. 1975). Predictions and data are normalized to match the total cross sections given by the fitted formula given by Dermer (1986b). The scaling calculation has been executed as a combination of the analytic Stephens and Badhwar (1981) model and a Monte Carlo program DECAY (Hänssgen and Ritter 1984) to treat π^0 decays. One sees a general agreement of data with Monte Carlo predictions, but some overprediction is seen in the forward and backward ($|y^*| \gtrsim 2$) directions at high energies. This tendency is more evident for PYTHIA: it may partly due to its main intention to describe high transverse momentum (p_T) phenomena, while FRITIOF is a model to describe low p_T hadronic reactions. We do not use PYTHIA to calculate the gamma-ray flux since the forward region plays an important role at high energies (see below).

Fig. 4 shows the comparison of the model prediction of the invariant cross section of π^0 production with experimental data at ISR. The differential cross sections of gamma-rays based on Monte Carlo programs have been converted to invariant cross sections of π^0 's using Sternheimer relation (Sternheimer 1955) following the strategy given in Stephens and Badhwar (1981).⁵ Monte Carlo calculations agree well with the scaling calculations given by Stephens and Badhwar, but both of them overpredict the cross sections at higher rapidities, as was seen in the previous figure (see the discussion of Stephens and Badhwar about the significance of this discrepancy). This results in systematic uncertainties of the final gamma-ray flux at higher energies ($E_\gamma \gtrsim 100$ GeV).

2.2. Inclusive cross section

Measured inclusive cross sections, $\langle \zeta \sigma_\pi(T_p) \rangle$, for the reaction $p + p \rightarrow \pi^0 + \text{anything}$ are well fitted by the analytic parameterization given by Dermer (1986b) for $T_p \leq 1$ TeV. In order to extend the calculation to higher energies, inclusive cross sections have been computed with a help of Monte Carlo simulators. In order to match the experimental data, inclusive cross sections of π^0 production are computed from inclusive cross sections of gamma-ray production assuming all gamma-rays are from π^0 decays. Fig. 5 compares experimental results with the Dermer's parameterization and the PYTHIA and FRITIOF prediction. Total p - p cross sections are calculated by a parameterization inspired by Regge theory (Donnachie and Landshoff 1992) in PYTHIA and by a Block-Cahn fit (Block and Cahn 1987) in FRITIOF. We adopt Dermer's parameterization below 1 TeV/c and use $163(s/1876 \text{ GeV}^2)^{0.21}$ mb as a smooth fit to the PYTHIA prediction above 1 TeV/c, where $s = 2m_p(T_p + 2m_p)$ with m_p the proton mass, since it is based on newer fit to the total cross section and charged particle multiplicity distributions are described well up to $\sqrt{s} = 900$ GeV (Sjöstrand and van Zijl 1987).

⁵ We have used the correct formula: $E(d^3\sigma/dp^3) = -(1/2)(\partial/\partial p)(d^2\sigma/(dpd\Omega)) \approx (1/2)(B + 2C)(d^2\sigma/(dpd\Omega))$ if $d^2\sigma/(dpd\Omega) \propto \exp(-Bp - Cp^2)$.

2.3. Cosmic-ray proton flux

Galactic diffuse gamma-rays are mostly produced in the central region of the Galaxy and we should use the cosmic-ray spectrum there: however, since our knowledge is limited within the local solar neighborhood, the best we can do is to use the local cosmic-ray spectrum which is estimated by using appropriate assumptions from the solar-modulated spectrum actually observed. Fig. 6 summarizes the observations and demodulated spectra calculated by different authors. There is a factor of about 5 uncertainty in the proton spectrum at $T_p = 1$ GeV, but as we will see these low energy protons do not contribute much to the diffuse flux, as has been pointed out before (e.g. Stephens and Badhwar 1981). In order to quantify the spectrum uncertainty, we will calculate the diffuse gamma-ray flux for three extreme cases: the “maximal” (“minimal”) flux corresponds to the upper (lower) envelope of calculated demodulated spectra and connects to $E^{-2.75}$ spectra above 100 GeV, and the “median” flux takes the form of

$$J_p(T_p) = \begin{cases} 1.67 p_p^{-2.7} \left[1 + \left(\frac{2.5 \text{ GeV}/c}{p_p} \right)^2 \right]^{-1/2} & (E_p \leq 100 \text{ GeV}) \\ 6.65 \times 10^{-6} \left(\frac{E_p}{100 \text{ GeV}} \right)^{-2.75} & (E_p > 100 \text{ GeV}) \end{cases} \quad (3)$$

where $E_p = T_p + m_p$, $p_p = \sqrt{E_p^2 - m_p^2}$ and the unit is $\text{cm}^{-2}\text{s}^{-1}\text{sr}^{-1}$. These are inspired by the parameterization on the demodulated spectrum given by Ormes and Protheroe (1983) for $E_p \leq 100$ GeV and the fit by Honda et al. (1995) for higher energies. The cosmic-ray proton fluxes used in this work are shown in Fig. 7. Notice that these fluxes are *extremes* and do not represent *typical* errors. Since the direct observation of cosmic-ray composition is limited to energies less than 10^6 GeV/nucleus, and there may be a possible steepening of the proton flux above 40 TeV (Asakimori et al. 1993), flux of diffuse gamma-rays above about 10^4 GeV suffers large uncertainty.

2.4. Effect of heavier nuclei

The effect of heavier nuclei than proton in cosmic-ray and the interstellar matter was estimated by different authors. It has been treated as a constant multiplication factor independent of energy. This is valid for the calculation of diffuse gamma-rays in the GeV region, since the proton/helium ratio in cosmic-rays seems to be constant in the 10~100 GeV range. However, recent observations show different spectral indices between protons and other heavier nuclei (see Biermann, Gaisser and Stanev 1994; Wiebel-Sooth, Bierman and Meyer 1995 for summary). This difference may be explained by a model in which protons and heavier nuclei come from different kinds of sources (Biermann, Gaisser and Stanev 1994). Therefore we derive an energy dependence of this nuclear enhancement factor, ϵ^M , assuming $E^{-2.75}$ spectrum for protons and $E^{-2.63}$ spectra for heavier nuclei (Wiebel-Sooth, Bierman and Meyer 1995). Following Gaisser and Shaefer (1992),

ϵ^M can be written as

$$\epsilon^M = \sum_i^{\text{CR}} \left(\frac{n_i}{n_p} \right)_{\text{CR}} \frac{1}{2} \left[w_{ip} \frac{\sigma_{ip}}{\sigma_{pp}} + \frac{\sigma_{i\alpha}}{\sigma_{pp}} \left(\frac{n_\alpha}{n_H} \right)_{\text{ISM}} w_{i\alpha} \right], \quad (4)$$

dropping a factor which is related to propagation (only necessary for the case of antiprotons discussed in Gaisser and Shaefer (1992), where $(n_i/n_p)_{\text{CR}}$ is the ratio of numbers of nuclei of type i to protons (the subscript CR indicates the quantity in cosmic-rays), $w_{ip}(w_{i\alpha})$ the total number of wounded nucleons in a collision between a nucleus i and a proton (α), $\sigma_{ip}(\sigma_{i\alpha})$ the total inelastic cross section for a collision between a nucleus i and a proton (α), and $(n_\alpha/n_H)_{\text{ISM}}$ is the ratio of helium to hydrogen in interstellar matter (ISM). The ISM is assumed to be a mixture of 93% hydrogen and 7% helium after Garcia-Munoz et al. (1987). We assume

$$\left(\frac{n_i}{n_p} \right)_{\text{CR}} = \left(\frac{n_i}{n_p}(\text{GeV}) \right)_{\text{CR}} \times \begin{cases} 1 & (i = p \text{ or } T_p \leq 100 \text{ GeV}) \\ \left(\frac{T_p}{100 \text{ GeV}} \right)^{0.12} & (\text{otherwise}). \end{cases} \quad (5)$$

where $(n_i/n_p(\text{GeV}))_{\text{CR}}$ is the cosmic-ray abundance in GeV range and is tabulated in Gaisser and Shaefer (1992). The result is plotted in Fig. 8 which is to be compared with previous estimates: 1.5 by Cavallo and Gould (1971), 1.6 ± 0.1 by Stephens and Badhwar (1981), 1.45 by Dermer (1986a). ϵ^M takes a value of 1.52 for $T_p < 100$ GeV, as given in Gaisser and Shaefer (1992). Notice that in the above expression the relativistic rise of interaction cross sections is cancelled out. The differences may be partly attributed to a larger multiplicity enhancement factor used in Stephens and Badhwar (1981) and a lower helium/proton ratio used in Dermer (1986a).

2.5. Monte Carlo calculation

Monte Carlo simulators can produce gamma-rays as final products instead of π^0 's, including the decay kinematics. Also other secondaries, such as neutral kaons which may yield gamma-rays, are included, although their contribution is minor. Thus we generated histograms for gamma-rays, not for π^0 's, for various proton energies with logarithmic binning (1 decade = 10 bins). In this case the equation (1) can be written in a summation form of

$$q(E_{\gamma,j}) \cdot \Delta E_\gamma = 4\pi n_H \sum_i \Delta T_{p,i} j_p(T_{p,i}) \langle \zeta \sigma_\pi(T_{p,i}) \rangle f(T_{p,i}; E_{\gamma,j}), \quad (6)$$

or, using $\Delta E_{\gamma,j} = E_{\gamma,j} \Delta$ and $\Delta T_{p,i} = T_{p,i} \Delta$ where $\Delta = 10^{0.05} - 10^{-0.05}$,

$$q(E_{\gamma,j}) = 4\pi n_H \sum_i j_p(T_{p,i}) \langle \zeta \sigma_\pi(T_{p,i}) \rangle f(T_{p,i}) T_{p,i} / E_{\gamma,j} \quad (7)$$

with $f(T_{p,i}; E_{\gamma,j})$ the normalized value of the histograms at $E_{\gamma,j}$ ($\sum_i f(T_{p,i}; E_{\gamma,j}) = 2$ here to incorporate the fact that 2γ 's are produced by a π^0). In the range of energies $3 \text{ GeV} < T_p < 12.5 \text{ GeV}$ no complete experimental data are available. Therefore we decided to use HADRIN for $T_p \leq 8$

GeV, the scaling model for $T_p \geq 3$ GeV, and FRITIOF for $T_p > 10$ GeV: we joined models with a linear connection in the overlapping energy regions (3–8 GeV) to obtain a smooth curve. Above 10 GeV results from two models will be compared. For Monte Carlo programs 80,000~1,000 events were generated for incident proton energies of $T_p = 10^{-0.5}, 10^{-0.4}, 10^{-0.3}, \dots, 10^{6.9}, 10^7$ GeV, respectively, depending on energy in order to have enough statistical accuracy while saving computing time.

3. Results

Fig. 9 shows our results on the emissivity of gamma-rays from the interaction of cosmic-rays with unit density of atomic hydrogen for two interaction models for $T_p \geq 10$ GeV, the scaling model and FRITIOF. The statistical errors due to Monte Carlo calculations are (typically): 4, 0.6, 0.8, 2, and 3% at $E_\gamma = 0.01, 0.1, 1, 10, \text{ and } 100$ GeV, respectively. For the cosmic-ray proton flux, we assumed three cases: “median”, “maximum”, and “minimum”. (For FRITIOF we only show the result with the “median” flux.) The “maximal” (“minimal”) proton flux gives about 50% higher (lower) gamma-ray flux at around 0.1 GeV and about 20% at around 10 GeV compared with that with the “median” flux. Remembering that these are *extremes*, we may say that the *standard* uncertainty of the calculated flux derived from the uncertainty of cosmic-ray proton flux is around 20 to 30%. The calculated emissivity is 34% higher at 10 GeV when we use FRITIOF compared with the scaling model: this may be a measure of systematic uncertainty related to the interaction model of the present prediction.

Table 1 summarizes the calculated gamma-ray emissivities for three cases of the cosmic-ray proton flux in differential and integral form with the scaling model.

Table 1. Gamma-ray emissivity due to secondary particle production in collisions of cosmic-rays with interstellar matter.

Energy in GeV	Differential rate in photon s ⁻¹ GeV ⁻¹ n _H ⁻¹			Integral rate in photon s ⁻¹ n _H ⁻¹		
	minimum	median	maximum	minimum	median	maximum
1.000E-02	5.872E-26	9.960E-26	1.380E-25	9.335E-26	1.646E-25	2.385E-25
1.585E-02	1.133E-25	2.019E-25	2.924E-25	9.298E-26	1.639E-25	2.376E-25
2.512E-02	1.894E-25	3.540E-25	5.358E-25	9.188E-26	1.619E-25	2.347E-25
3.981E-02	2.478E-25	4.726E-25	7.298E-25	8.915E-26	1.568E-25	2.268E-25
6.310E-02	2.721E-25	5.223E-25	8.124E-25	8.384E-26	1.466E-25	2.112E-25
1.000E-01	2.581E-25	4.937E-25	7.652E-25	7.495E-26	1.296E-25	1.847E-25
1.585E-01	2.088E-25	3.937E-25	6.006E-25	6.206E-26	1.050E-25	1.467E-25
2.512E-01	1.333E-25	2.413E-25	3.549E-25	4.651E-26	7.594E-26	1.027E-25
3.981E-01	6.908E-26	1.175E-25	1.630E-25	3.164E-26	4.940E-26	6.416E-26
6.310E-01	3.206E-26	5.116E-26	6.684E-26	1.977E-26	2.949E-26	3.690E-26
1.000E+00	1.301E-26	1.961E-26	2.447E-26	1.131E-26	1.618E-26	1.971E-26
1.585E+00	4.765E-27	6.861E-27	8.314E-27	5.986E-27	8.229E-27	9.847E-27
2.512E+00	1.546E-27	2.125E-27	2.524E-27	2.982E-27	3.946E-27	4.681E-27
3.981E+00	4.812E-28	6.348E-28	7.494E-28	1.455E-27	1.866E-27	2.216E-27
6.310E+00	1.497E-28	1.910E-28	2.266E-28	7.027E-28	8.805E-28	1.052E-27
1.000E+01	4.579E-29	5.698E-29	6.822E-29	3.324E-28	4.108E-28	4.934E-28
1.585E+01	1.361E-29	1.673E-29	2.016E-29	1.539E-28	1.894E-28	2.280E-28
2.512E+01	3.952E-30	4.854E-30	5.852E-30	7.028E-29	8.672E-29	1.041E-28
3.981E+01	1.133E-30	1.398E-30	1.678E-30	3.192E-29	3.955E-29	4.731E-29

At this stage it may be worth showing the contributions of cosmic-ray protons of various energies to gamma-rays of some specific energies in Fig. 10. From this figure one can see most diffuse gamma-rays below about 300 MeV of nuclear origin come from protons with kinetic energies of a few to several GeV, where no experimental results for secondary pion production are available and where there is a large uncertainty in the cosmic-ray proton flux.

The results obtained here are compared with previous calculations (Cavallo and Gould 1971, Stecker 1979, Stephens and Badhwar 1981, Dermer 1986a) in Figs. 11 and 12, where in the latter they are plotted in integrated form: $q(> E_\gamma) = \int_{E_\gamma}^{\infty} q(E'_\gamma) dE'_\gamma$. The main difference between authors may come from the assumed demodulated spectrum of the cosmic-ray protons. (See Fig. 1 of Dermer (1986a) for comparison of assumed spectra.)

We can extend our calculation to higher energy gamma-rays and the results are presented in Fig. 13 with previous calculations (Stecker 1979, Berezhinsky et al. 1993, Chardonnet et al. 1995). For this plot we show calculation only with the scaling model: FRITIOF causes fatal errors at $\gtrsim 10$ TeV. Since the mean interaction length of gamma-rays for photon-photon collisions with the cosmic microwave background radiation becomes comparable to the distance to the Galactic center from Earth above several 100 TeV (Protheroe 1986), gamma-ray flux at higher energies than this are greatly reduced. Thus we stop our calculation at 100 TeV. The proton fluxes used in other calculations are: $2.35E_p^{-2.67}$ (Stecker) and $1.75E_p^{-2.73}$ (Chardonnet et al.), where E_p is in GeV and the unit is $\text{cm}^{-2}\text{s}^{-1}\text{sr}^{-1}\text{GeV}^{-1}$. Berezhinsky et al. assumed the *total* cosmic-ray spectrum to be $1.59E_p^{-2.73} \text{ cm}^{-2}\text{s}^{-1}\text{sr}^{-1}(\text{GeV/nucleon})^{-1}$. Also shown is the effect of energy-dependent nuclear enhancement factor (ϵ^M), which raise the expected flux by about 10% at 1 TeV. The flux given in Berezhinsky et al. is smaller than others, partly due to the assumed cosmic-ray spectrum.

In Table 2 the integral gamma-ray emissivities calculated by different authors are summarized.

4. Discussion

Now we compare our results with the EGRET data (Hunter et al. 1996).

Fig. 14 shows the Galactic diffuse gamma-ray flux in a differential form, multiplied by E_γ^2 to make the differences more visible. The dotted line shows the expectation as the sum of three components of diffuse gamma-rays: cosmic-ray nuclear interactions (which is the main concern of this paper and is dominant above about 200 MeV), electron bremsstrahlung, and inverse Compton. The components were calculated by the model developed by Hunter et al. (1996), which incorporates the detailed distribution of interstellar matter, and are averaged over the Galactic center region, $300^\circ < \ell < 60^\circ$, $|b| \leq 10^\circ$. In their model they used the gamma-ray emissivity from cosmic-ray interactions given by Stecker (1988). Solid and dashed lines are the expected fluxes in which the gamma-ray emissivity is replaced with the ones computed in this work: solid line assumes the “median” proton flux and dashed lines assume the “minimal” and “maximal” fluxes. None of the models mentioned above seems to yield enough gamma-rays above 1 GeV: thus we

Table 1—Continued

Energy in GeV	Differential rate in photon $\text{s}^{-1}\text{GeV}^{-1}n_{\text{H}}^{-1}$			Integral rate in photon $\text{s}^{-1}n_{\text{H}}^{-1}$		
	minimum	median	maximum	minimum	median	maximum
6.310E+01	3.238E-31	4.015E-31	4.799E-31	1.451E-29	1.804E-29	2.151E-29
1.000E+02	9.277E-32	1.153E-31	1.375E-31	6.625E-30	8.248E-30	9.820E-30
1.585E+02	2.669E-32	3.324E-32	3.956E-32	3.039E-30	3.788E-30	4.505E-30
2.512E+02	7.721E-33	9.626E-33	1.145E-32	1.403E-30	1.750E-30	2.079E-30
3.981E+02	2.248E-33	2.805E-33	3.333E-33	6.514E-31	8.129E-31	9.656E-31
6.310E+02	6.590E-34	8.224E-34	9.768E-34	3.042E-31	3.797E-31	4.509E-31
1.000E+03	1.941E-34	2.423E-34	2.878E-34	1.427E-31	1.782E-31	2.115E-31
1.585E+03	5.747E-35	7.175E-35	8.518E-35	6.724E-32	8.395E-32	9.967E-32
2.512E+03	1.708E-35	2.133E-35	2.532E-35	3.180E-32	3.971E-32	4.714E-32
3.981E+03	5.098E-36	6.365E-36	7.556E-36	1.510E-32	1.885E-32	2.238E-32
6.310E+03	1.527E-36	1.906E-36	2.263E-36	7.188E-33	8.976E-33	1.065E-32
1.000E+04	4.587E-37	5.727E-37	6.798E-37	3.432E-33	4.285E-33	5.086E-33
1.585E+04	1.383E-37	1.726E-37	2.049E-37	1.642E-33	2.050E-33	2.434E-33
2.512E+04	4.181E-38	5.221E-38	6.197E-38	7.863E-34	9.819E-34	1.165E-33
3.981E+04	1.269E-38	1.585E-38	1.881E-38	3.759E-34	4.694E-34	5.572E-34
6.310E+04	3.856E-39	4.816E-39	5.716E-39	1.784E-34	2.227E-34	2.644E-34
1.000E+05	1.153E-39	1.440E-39	1.709E-39	8.340E-35	1.042E-34	1.236E-34

Note. — Figures to be read as $5.782\text{E-}26 = 5.782 \times 10^{-26}$, etc. “Minimum”, “median” and “maximum” denote the models of the cosmic-ray spectrum (see text). The scaling model is used for $T_p \geq 10$ GeV.

may conclude that even the detailed model studied here cannot explain the excess of Galactic diffuse gamma-ray flux above 1 GeV.

As one of the possible solutions to the problem, we tried to fit the cosmic-ray proton spectrum from the EGRET data with a single power-law spectrum in total energy, $J_p(E_p) = aE_p^{-b}$, and have computed the χ^2 's in the a - b plane and searched the minimum.

The results are $a = 1.48_{-0.20}^{+0.17} \text{ cm}^{-2}\text{s}^{-1}\text{sr}^{-1}\text{GeV}^{-1}$ and $b = 2.45_{-0.04}^{+0.03}$ when we use the scaling model for $T_p \geq 10 \text{ GeV}$ ($a = 1.67_{-0.20}^{+0.23} \text{ cm}^{-2}\text{s}^{-1}\text{sr}^{-1}\text{GeV}^{-1}$ and $b = 2.51 \pm 0.04$ with FRITIOF for $T_p \geq 10 \text{ GeV}$). The expected flux calculated from this best fit is plotted in Fig. 14 as a dotdashed line. This spectrum gives a better fit above 1 GeV, but predicts higher gamma-ray flux than observed around several 100 MeV.

However, this flatter proton spectrum is not consistent with the direct observations above 10 GeV (see Fig. 7). Therefore one may be tempted to suggest a possibility that the cosmic-ray spectrum is flatter in the Galactic center region than the one in the local (solar neighborhood) region. It is interesting to note that the power-law index obtained here is similar to that of the cosmic-ray source spectrum predicted by the cosmic-ray reacceleration theory (Ptuskin 1995 and references therein): in this theory the source spectrum is proportional to $R^{-\gamma_s}$, where $\gamma_s = 2.3 \sim 2.4$ (where R is the rigidity) and the escape length to $R^{-1/3}$ to match the observed spectrum at all energies.

In any case, more detailed analysis is necessary before going on, since in the above fitting the bremsstrahlung and inverse Compton components are fixed: these components will change following the electron spectrum which is related to the proton spectrum through the cosmic-ray proton to electron ratio, which is usually believed to be universal.

On the other hand, *COS B* data indicate that the diffuse gamma-ray spectrum in the inner Galaxy ($310^\circ < \ell < 50^\circ$) is consistent with the cosmic-ray proton spectrum of about $\propto E_p^{-2.7}$ (Bloemen 1987), which does not seem to be consistent with the EGRET result (Hunter et al. 1996).

Further observations, including analysis of the EGRET data at high latitudes (Sreekumar et al. 1996), are necessary to resolve the spectral variation problem.

5. Conclusion

The gamma-ray spectrum from the decay of secondary neutral pions produced by interactions of cosmic-ray protons with interstellar gas has been calculated utilizing modern event generators which simulate high-energy p - p collisions by Monte Carlo methods. The result is not inconsistent with previous calculations: the observed excess of the Galactic diffuse gamma-rays above about 1 GeV can not be explained by revising the models of cosmic-ray interaction with interstellar matter. This might suggest flatter cosmic-ray proton spectra in the central region of the Galaxy

than in the solar neighborhood, but requires further study.

I gratefully acknowledge the EGRET team for the kind hospitality during my stay at NASA/GSFC, especially Dr. Stan Hunter for discussions and providing me the EGRET diffuse gamma-ray fluxes prior to publication, and Dr. Robert Hartman for his continuous encouragement and support. I also thank Drs. Jonathan Ormes, Charles Dermer, and Felix Aharonian for valuable discussions and suggestions.

REFERENCES

- Andersson, B., Gustafson, G. & Pi, H. 1993, *Z. Phys. C*, 57, 485
- Asakimori, K. et al. 1993, in *Proc. of the 23rd International Cosmic Ray Conference, Calgary*, 2, 21
- Badhwar, G. D., Stephens, S. A. & Golden, R. L. 1977, *Phys. Rev. D*, 15, 820
- Berezinsky, V. S. et al. 1993, *Astropart. Phys.*, 1, 281
- Bertsch, D. L. et al. 1993, *ApJ*, 416, 587
- Biermann, P. L., Gaisser, T. K. & Stanev, T. 1994, *Phys. Rev. D*, 51, 3450
- Block, M. & Cahn, R. N. 1987, *Phys. Lett. B*, 188, 143
- Bloemen, J. B. G. M. 1987, *ApJ*, 317, L15
- Bugg, D. V. et al. 1964, *Phys. Rev.*, 133, B1017
- Cavallo, G. & Gould, R. J. 1971, *Nuovo Cim.*, 2B, 77
- Chardonnet, P. et al. 1995, *ApJ*, 454, 774
- Dermer, C. D. 1986a, *A&A*, 157, 223
- Dermer, C. D. 1986b, *ApJ*, 307, 47
- Donnachie, A. & Landshoff, P. V. 1992, *Phys. Lett. B*, 296, 227
- Gaisser, T. K. & Shaefer, R. K. 1992, *ApJ*, 394, 174
- Garcia-Munoz, M. et al. 1987, *ApJS*, 64, 269
- Gloeckler, G. & Jokipii, J. R. 1967, *ApJ*, 148, L41
- Hänssgen, K. & Ritter, S. 1984, *Comput. Phys. Comm.* 31, 37
- Hänssgen, K. & Ranft, J. 1986, *Comput. Phys. Comm.* 39, 53
- Honda, M. et al. 1995, *Phys. Rev. D*, 52, 4985
- Hunter, S. D. et al. 1996, submitted to *ApJ*
- Ip, W.-H. & Axford, W. I. 1985, *A&A*, 149, 7

- Jaeger, K. et al. 1975a, *Phys. Rev. D*, 11, 1757
- Jaeger, K. et al. 1975b, *Phys. Rev. D*, 11, 2405
- Ivanenko, I. P. et al. 1993, in *Proc. of the 23rd International Cosmic Ray Conference, Calgary*, 2, 25
- Kawamura, Y. et al. 1989, *Phys. Rev. D*, 40, 729
- Nagashima, K. et al. 1989, *Nuovo Cim.*, 12C, 173
- Ormes, J. F. & Protheroe, R. J. 1983, *ApJ*, 272, 756
- Pi, Hong 1992, *Comput. Phys. Comm.* 71, 173
- Protheore, R. J. 1986, *MNRAS*, 221, 769 and references therein
- Ptuskin, V. S., 1995, rapporteur talk in *Proc. of the 24th International Cosmic Ray Conference, Rome*
- Ryan, M. J. et al. 1972, *Phys. Rev. Lett.*, 28, 985
- Seo, E. S. et al. 1991, *ApJ*, 378, 763
- Sheng, A. et al. 1975, *Phys. Rev. D*, 11, 1733
- Simpson, J. A. 1983, *Ann. Rev. Nucl. Particle Phys.*, 33, 323
- Stöstrand, T. & van Zijl, M. 1987, *Phys. Rev. D*, 36, 2019
- Stöstrand, T. 1994, *Comput. Phys. Comm.* 82, 74
- Smith, L. H. et al. 1973, *ApJ*, 180, 987
- Sreekumar, P. et al. 1996, in preparation
- Stecker, F. W. 1970, *Ap&SS*, 6, 377
- Stecker, F. W. 1979, *ApJ*, 228, 919
- Stecker, F. W. 1988, in *Cosmic Gamma Rays, Neutrinos and Related Astrophysics*, ed. Shapiro, M. M. and Wefel, J. P. (Dordrecht: Reidel), 85
- Sternheimer, R. M. 1955, *Phys. Rev.* 88, 277
- Stephens, S. A. and Badhwar, G. D. 1981, *Ap&SS*, 76, 213
- Webber, W. R. et al. 1987, in *Proc. of the 20th International Cosmic Ray Conference, Moscow*, 1, 325
- Webber, W. R. & Potgieter, M. S. 1989, *ApJ*, 344, 779
- Wiebel-Sooth, B., Biermann, P. L. & Meyer, H. 1995, in *Proc. of the 24th International Cosmic Ray Conference, Rome*, edited by Iucci, N. et al., 2, 656.

Table 2. Integrated Galactic gamma-ray emissivity from cosmic-ray interactions with interstellar matter.

Reference	Model	$q(> E_\gamma)^a$			
		0	0.1 GeV	1 GeV	1 TeV
Cavallo and Gould 1971	Isobar + Phase space	2.4	1.8	0.13	...
Stephens and Badhwar 1981	Scaling	1.92–2.34	1.37–1.63	0.115–0.116	...
Dermer 1986a	Isobar + Scaling	2.02	1.53	0.159	...
Stecker 1988 ^b	Isobar + Scaling	1.97	1.59	0.209	...
Berezinsky et al. 1993	SIBYLL	0.76×10^{-6}
Chardonnet et al. 1995	PYTHIA	1.5×10^{-6}
This work ^c	HADRIN + Scaling	1.65	1.30	0.162	1.78×10^{-6}
		(0.94–2.39)	(0.75–1.85)	(0.113–0.197)	$((1.43–2.12) \times 10^{-6})$

^aUnits: 10^{-25} s^{-1} per hydrogen atom.

^bComputed using the parameterization given in Bertsch et al. (1993).

^cThe “median” proton flux is used. (Emissivities with the “minimal” and “maximal” proton fluxes are shown in parentheses.)

Fig. 1.— Comparison of the model predictions with experimental data of the secondary π^0 spectrum in the CMS, corresponding to LS proton kinetic energy $T_p = 0.97$ GeV. Solid histogram: HADRIN, dashed line: isobar model by Stecker (1970), dotted line: scaling model by Stephens and Badhwar (1981), and asterisks: data of Bugg et al. (1964).

Fig. 2.— Same as in Fig. 1, but with the secondary π^0 spectrum in the laboratory system (LS).

Fig. 3.— Comparison of the model prediction with experimental data of the rapidity distribution of secondary gamma-rays at LS proton momentum of 12.4, 205 and 300 GeV/c. Solid (dotted) histograms: FRITIOF (PYTHIA), dashed curves: combination of the scaling model by Stephens & Badhwar (1981) and DECAY. Calculations are normalized to the inclusive cross section given by Dermer (1986b). Data of Jaeger et al. (1975a), Jaeger et al. (1975b) and Sheng et al. (1975).

Fig. 4.— Comparison of the invariant cross section for the production of neutral pions as a function of pion momentum in CMS at different emission angles for various colliding beam energies. Data points and scaling calculation (solid lines) are taken from Stephens and Badhwar (1981). Solid (dotted) histograms are converted from FRITIOF (PYTHIA) results using the Sternheimer relation (see text).

Fig. 5.— Inclusive cross sections for the production of neutral pions in proton-proton collisions as a function of the incident proton momentum. The data points are from the compilation of Appendix A of Dermer (1986b) and the dashed lines are the fits by Dermer (1986b). The results of FRITIOF (PYTHIA) are plotted in dotted (dotdashed) lines and a fit used in this work is shown by a solid line.

Fig. 6.— Compilation of the demodulated cosmic-ray proton spectra calculated by different authors and the data on the cosmic-ray proton flux at high energies. Lines are the demodulated spectra (Gloeckler and Jokipii 1967, Stephens and Badhwar 1981, Simpson 1983, Ormes and Protheroe 1983, Ip and Axford 1985, Nagashima et al. 1989, Webber and Potgieter 1989, Seo et al. 1991) and symbols are the data at high energies (pluses, open circles, closed circles, squares, crosses, inverse triangles and triangles are from Ryan et al. 1972, Smith et al. 1973, Webber et al. 1987, Kawamura et al. 1989, Seo et al. 1991, Asakimori et al. 1993 and Ivanenko et al. 1993, respectively.) Also shown by thick solid line is the “median” flux used in this work. See also Fig. 7. (The upper and lower dashed lines correspond to the curves BS and Mu of Stephens and Badhwar (1981).)

Fig. 7.— The demodulated cosmic-ray proton spectra used in this work: “median”, “maximum”, “minimum” and “best fit”, where the “maximum” (“minimum”) is taken as the upper (lower) envelopes of different calculations and data shown in Fig. 6. “Best fit” is derived from the EGRET data (see text). Also shown are the spectra used in previous calculation (Stephens and Badhwar 1981, Dermer 1986a) of the gamma-ray emissivity. (The upper and lower dashed lines correspond to the curves BS and Mu of Stephens and Badhwar (1981).)

Fig. 8.— The nuclear enhancement factor, ϵ^M , as a function of the incident cosmic-ray proton

energy.

Fig. 9.— The gamma-ray production source function per unit density of atomic hydrogen from the interaction of the cosmic-ray with the interstellar medium for different models of high-energy p - p collisions. Solid and dotted lines are the results with the scaling model and FRITIOF, respectively, for $T_p > 10$ GeV assuming the “median” cosmic-ray proton flux. Both of them used the same model for $T_p \leq 10$ GeV (see text). Also shown are the results assuming the “minimal” and “maximal” proton fluxes with the scaling model.

Fig. 10.— The contributions of cosmic-ray protons of various energies to gamma-rays of some specific energies.

Fig. 11.— Comparison of the gamma-ray production source functions per unit density of atomic hydrogen from the interaction of the cosmic-ray with the interstellar medium by different authors. Triple-dot-dashed, dashed, dotdashed lines are differential emissivities multiplied by E_γ^2 given in Cavallo and Gould (1971), Stephens and Badhwar (1981), Dermer (1986a) and Stecker (1988), respectively (the dotted curve is drawn by the parameterization given in Bersch et al. (1993), which fits the results of Stecker (1988)), and the solid line is from this work with PYTHIA and the “median” proton flux.

Fig. 12.— Comparison of the integrated gamma-ray production source functions per unit density of atomic hydrogen from the interaction of the cosmic-ray with the interstellar medium by different authors. Notations are the same as in Fig. 9.

Fig. 13.— The gamma-ray production source functions per unit density of atomic hydrogen from the interaction of the cosmic-ray with the interstellar medium for different models of high-energy p - p collisions at high energies. Solid lines are the results with the scaling model and the “median” proton flux, dashed lines are similar but with a fixed nuclear enhancement factor ($\epsilon^M \equiv 1.52$). Also shown are previous calculations (Stecker 1979, Berezhinsky et al. 1993, Chardonnet et al. 1995).

Fig. 14.— The diffuse gamma-ray differential spectrum, multiplied by E_γ^2 , of the Galactic center region. Data are from EGRET observations (Hunter et al. 1996) averaged over $300^\circ < \ell < 60^\circ$, $|b| \leq 10^\circ$. The model predictions based on gamma-ray emissivities from cosmic-ray nuclear interactions with different assumptions are also shown. Solid line: the scaling model and the “median” proton flux, dashed lines: the scaling model and the “maximum” and “minimum” proton flux, and dotted line: from Hunter et al. (1996) based on the result of Stecker (1988). Also shown by dotdashed lines are spectra obtained with the scaling model and the “best fit” proton flux ($\propto E_p^{-2.45}$). See text for detail.

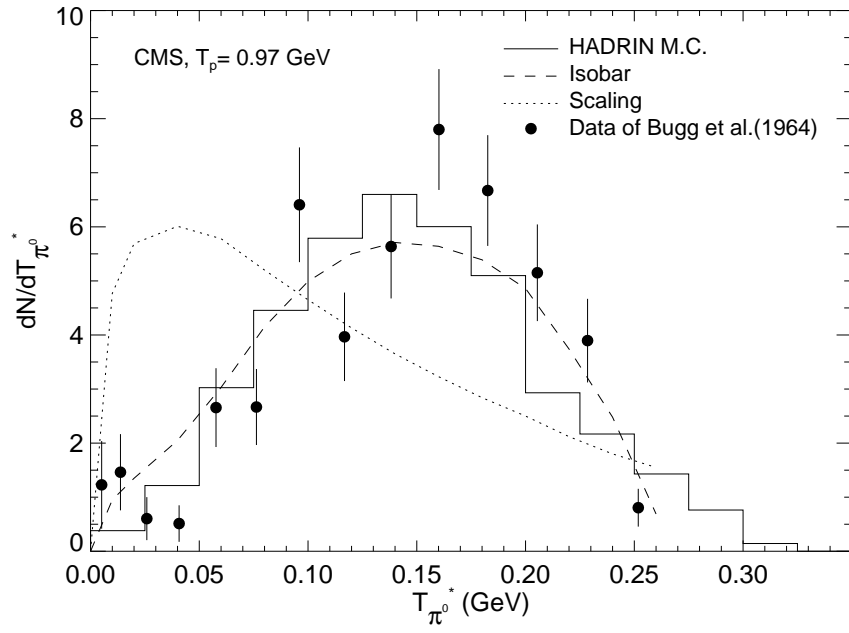


Fig. 1

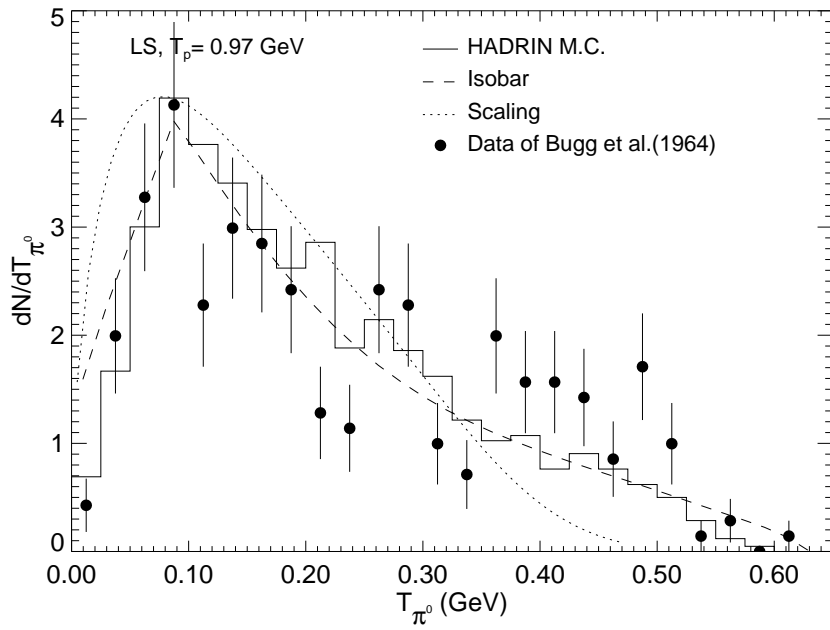


Fig. 2

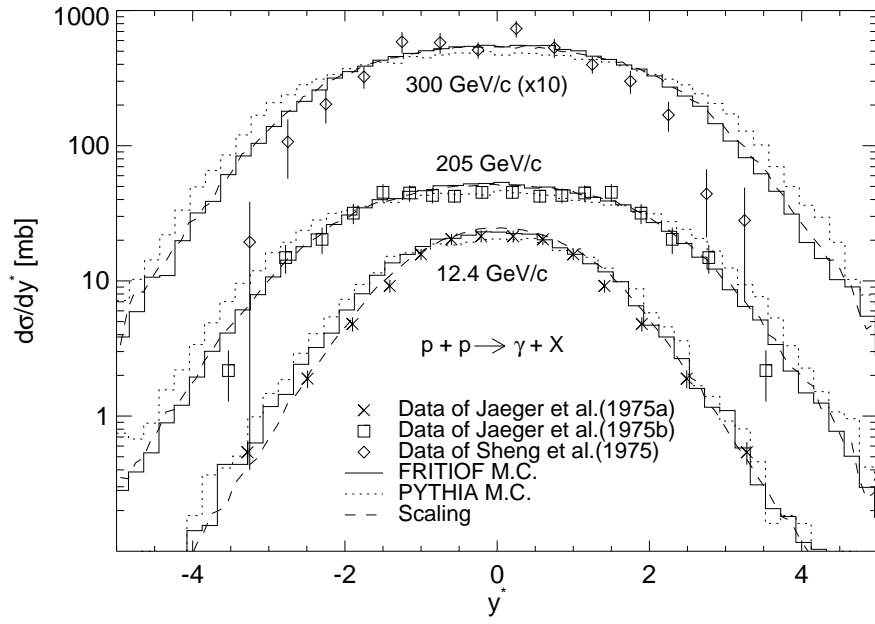


Fig. 3

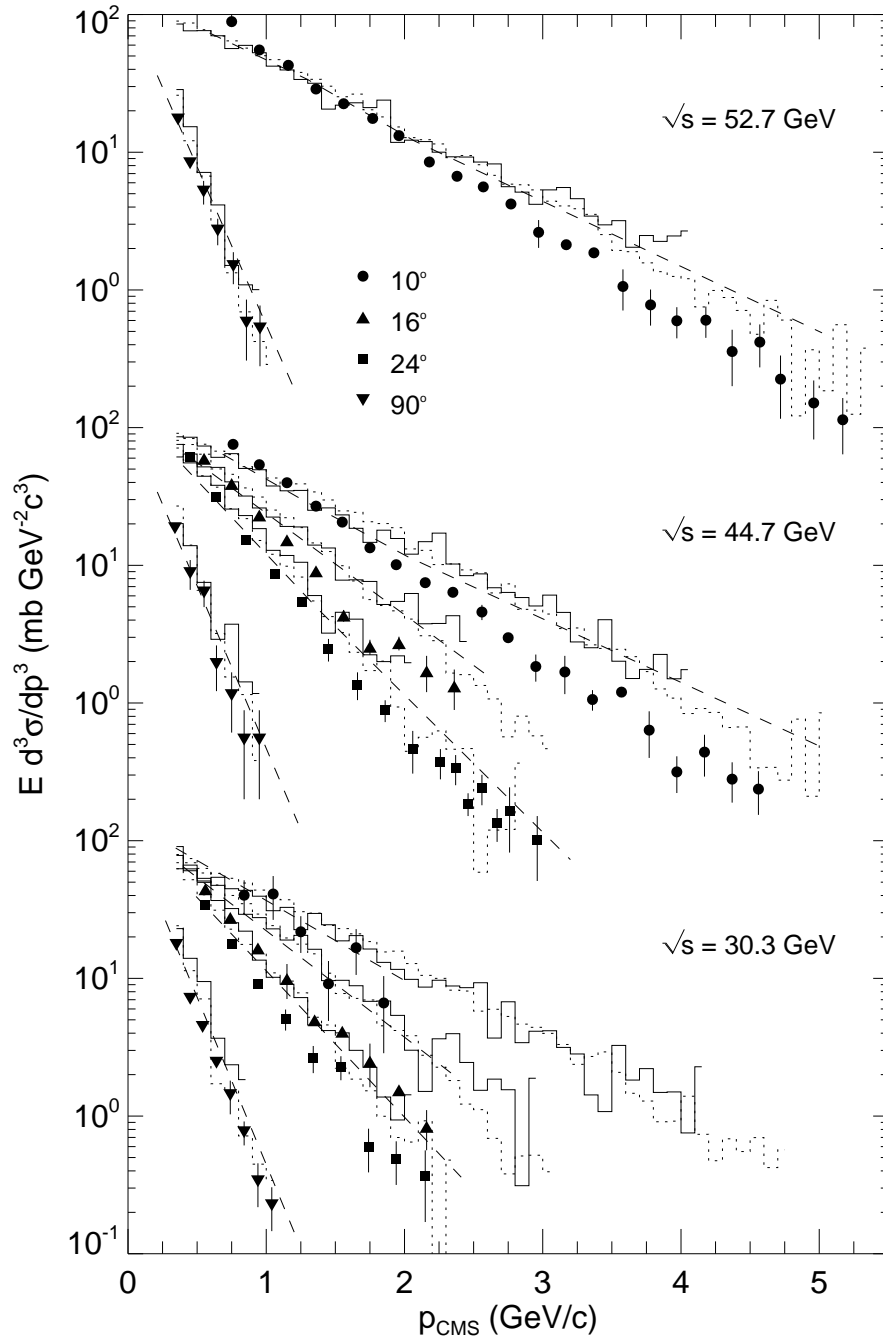


Fig. 4

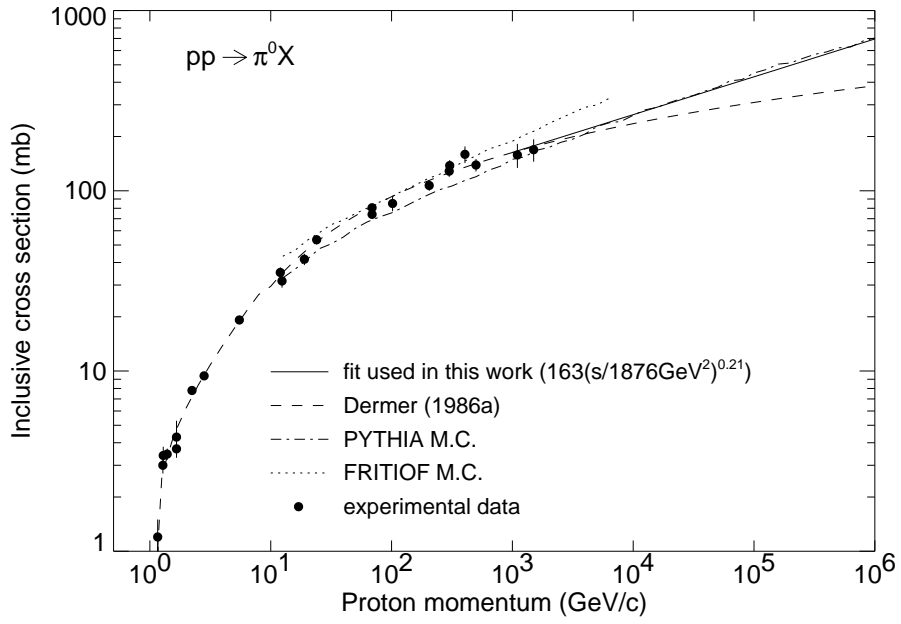


Fig. 5

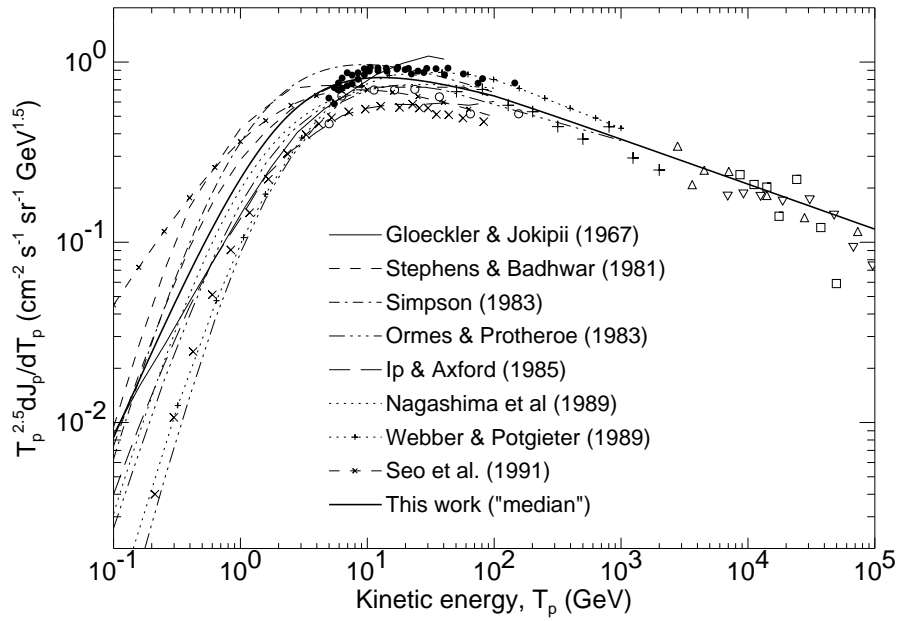


Fig. 6

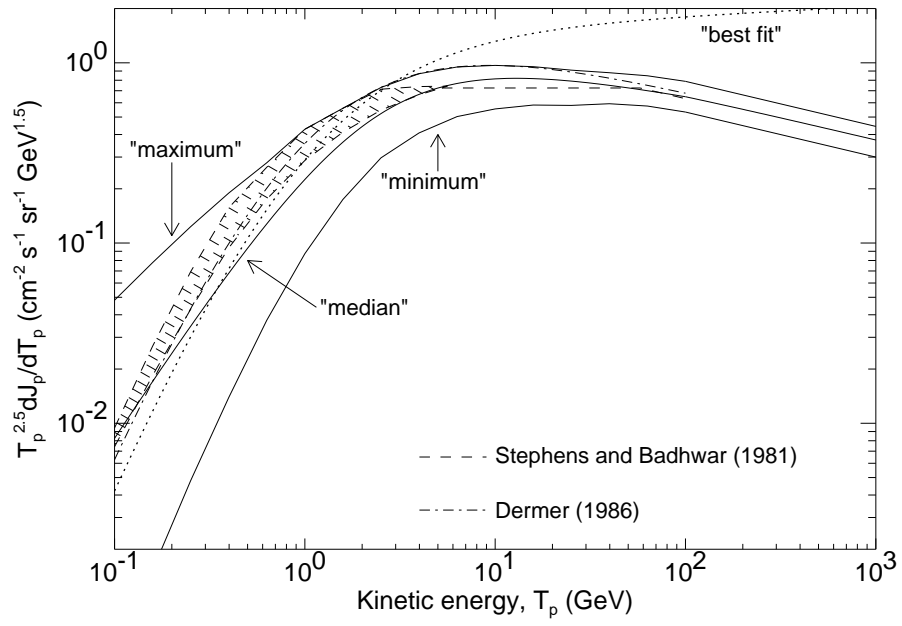


Fig. 7

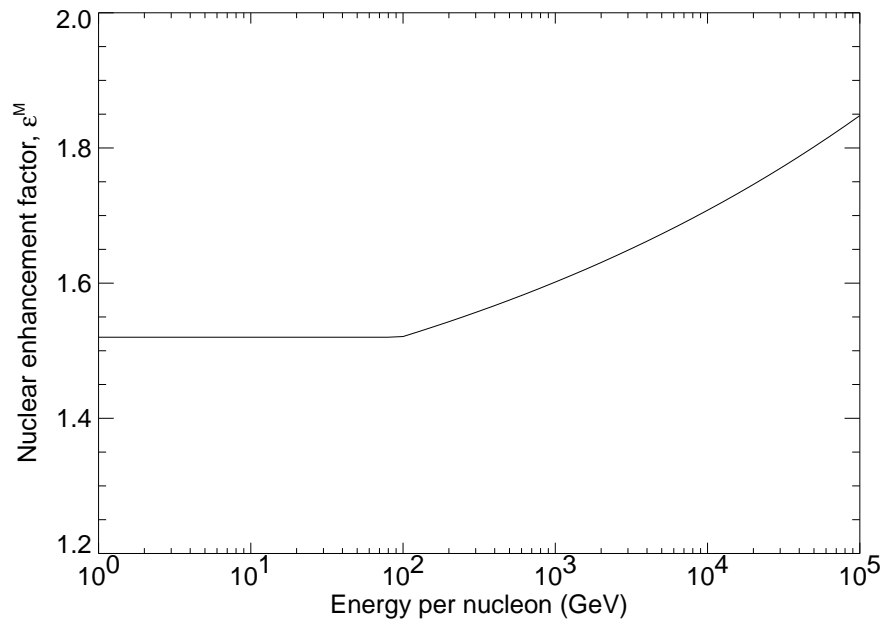


Fig. 8

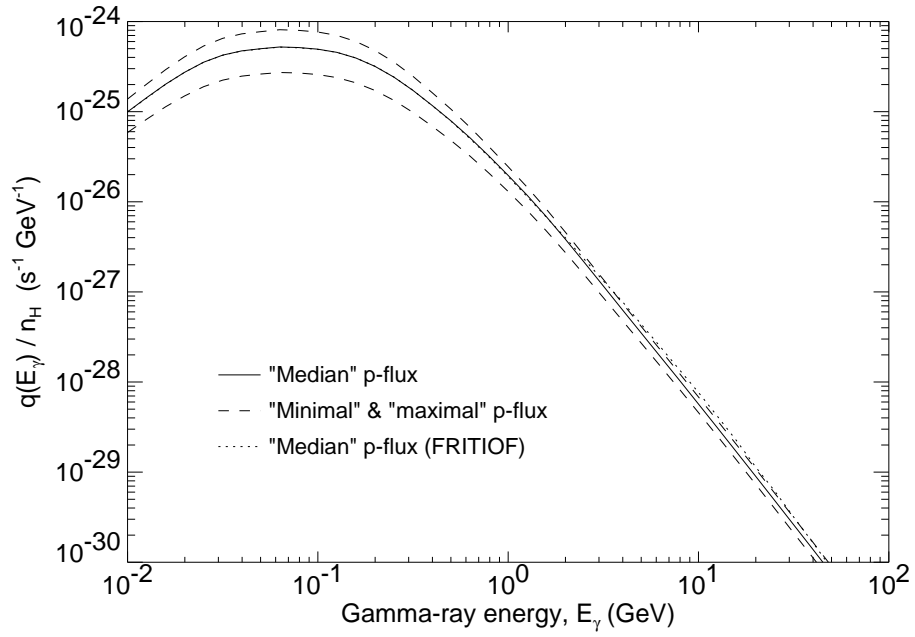


Fig. 9

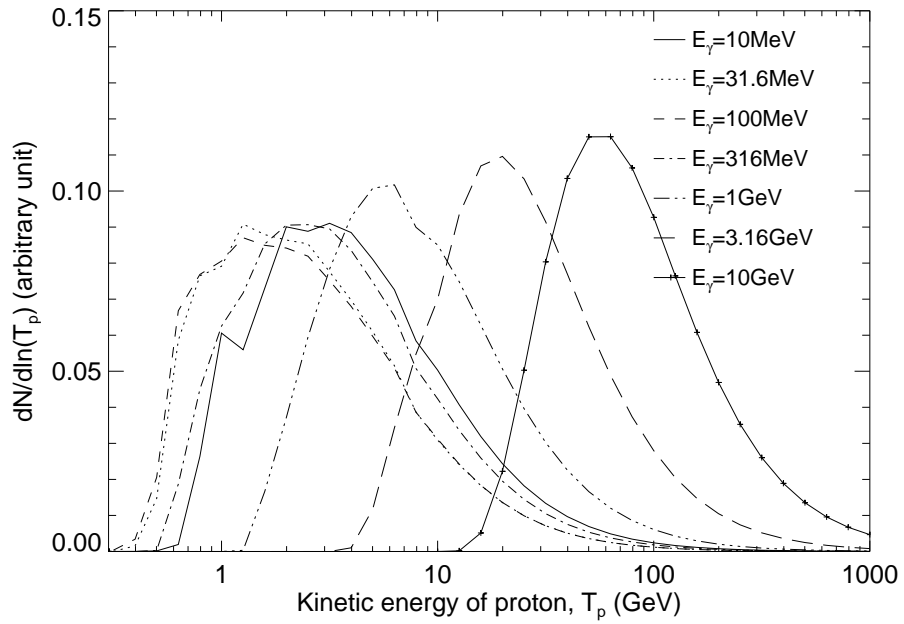


Fig. 10

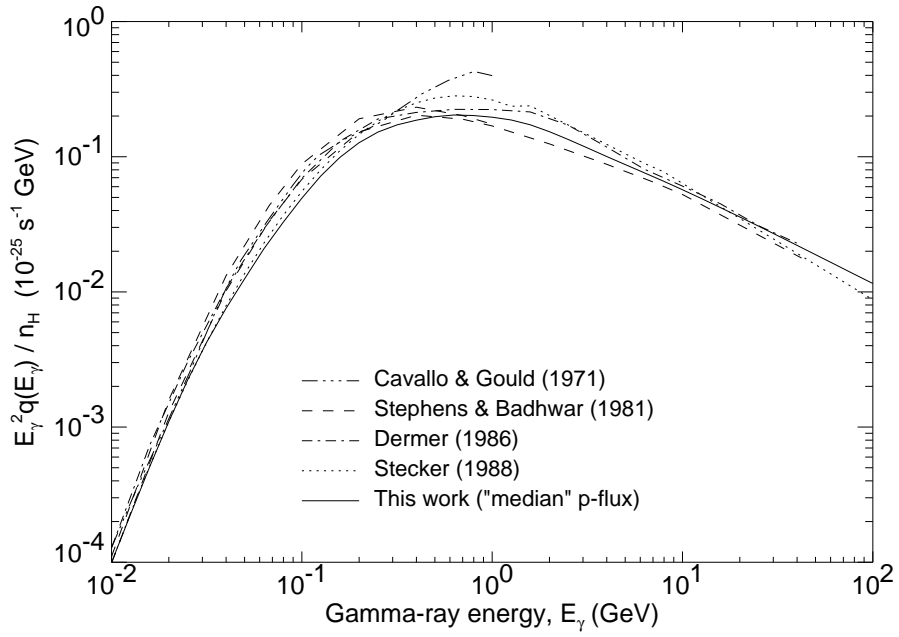


Fig. 11

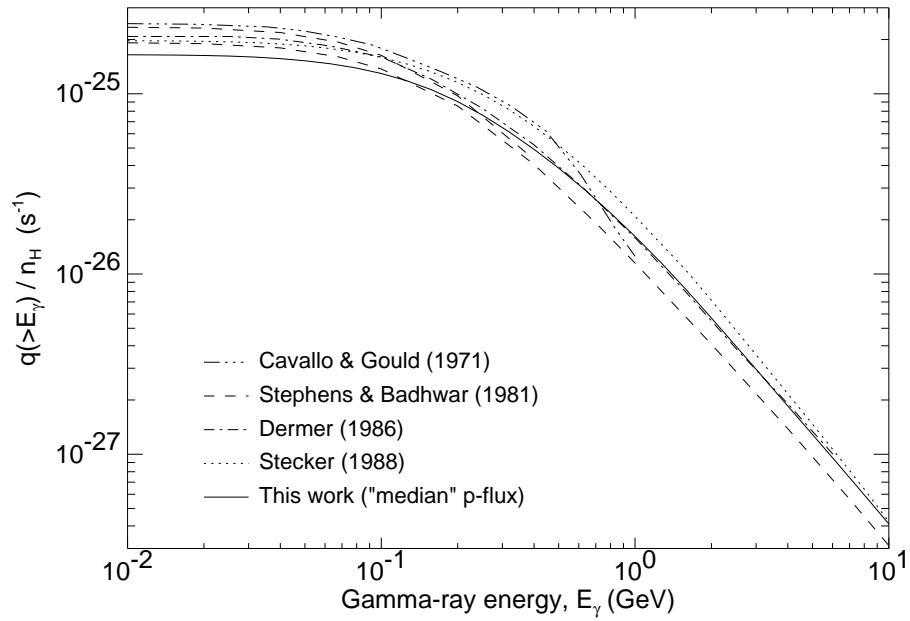


Fig. 12

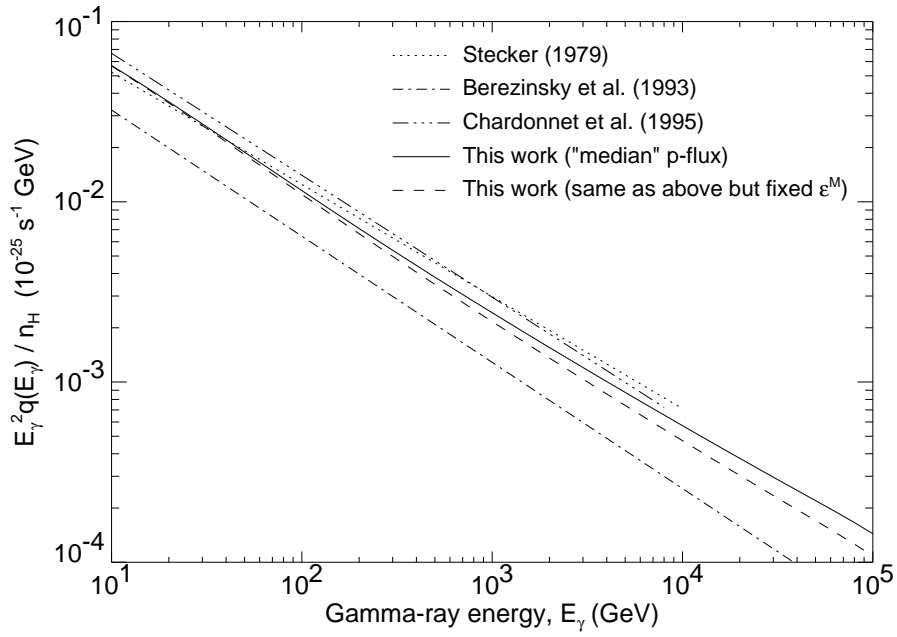


Fig. 13

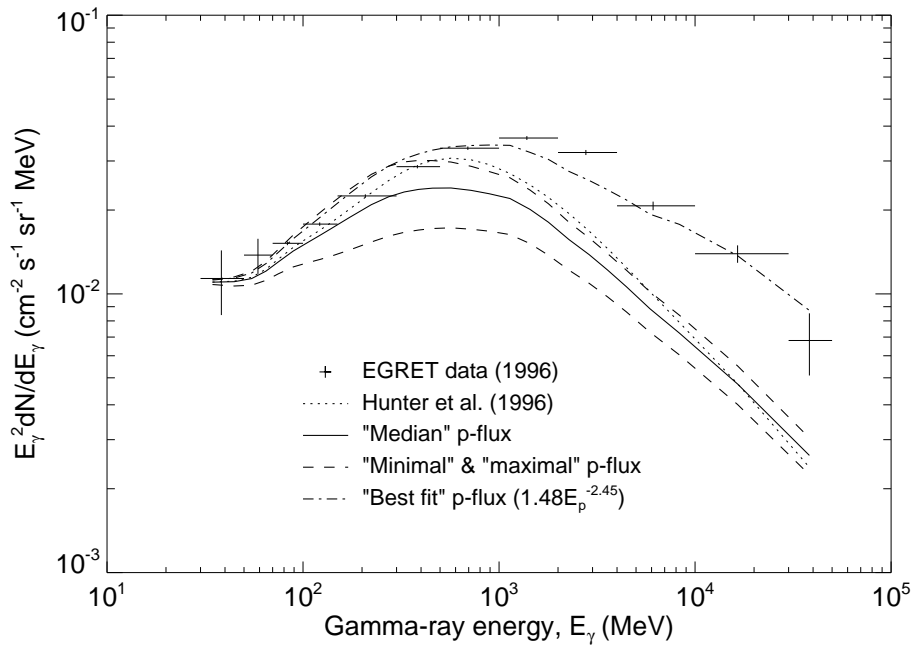


Fig. 14